https://doi.org/10.5194/egusphere-2024-2999
Preprint. Discussion started: 24 October 2024

The evolution of aerosols mixing state derived from a field campaign in Beijing: implications to the particles aging time scale in urban atmosphere

Jieyao Liu[1], Fang Zhang[2], Jingye Ren[3], Lu Chen[4]

[1] School of Geographical Sciences, Hebei Normal University, Shijiazhuang, China

[2] School of Civil and Environmental Engineering, Harbin Institute of Technology (Shenzhen), Shenzhen, China

[3] Xi'an Institute for Innovative Earth Environment Research, Xi'an, China

[4] Faculty of Geographical Science, Beijing Normal University, Beijing, China

Correspondence to: Fang Zhang (zhangfang2021@hit.edu.cn)

Abstract

The mixing states and aging time scale of aerosol particles play a vital role in evaluating their climate effects. Here, we identified four different real-time mixing patterns of size-resolved particles using the field measurement by a humidity tandem differential mobility analyzer (H-TDMA) in the urban Beijing. We show that the particles with external, transitional and internal mixing state during the campaign account for 20-48%, 17-24% and 27-56% respectively and the fraction highly depends on particles size. The diurnal variation of the mixing states of particles in all sizes investigated (40, 80, 110, 150 and 200 nm) present an apparent aging process from external to internal mixing state, typically spanning a duration of approximately 5–8 hours from 8:00–10:00 to 15:00–17:00. Additionally, the results illustrate that high ambient temperature during daytime or more humid atmosphere accelerates the aging process of aerosol particles, leading to the particles from external to internal mixing on both

https://doi.org/10.5194/egusphere-2024-2999
Preprint. Discussion started: 24 October 2024

clear and cloudy days. Also, with the evolution of particulate pollution, the aerosol particles become more internally-mixed. Our result implies that those fine aerosol particles experience aging through both the photochemical process and aqueous growth in the polluted atmosphere of urban Beijing. Furthermore, through a comprehensive review of the aging timescale of particles adopted in current models and derived from observations, we show the great discrepancy between observations and models, highlighting the importance to parameterize their aging time scale based on more field campaigns.

1 Introduction

The mixing state of atmospheric aerosol particles can affect the hygroscopicity and the ability to serve as cloud condensation nuclei (CCN), and thus the air quality and climate (Müller et al., 2017; Xu et al., 2021; Yao et al., 2022; Ge et al., 2024). It has been shown that the aerosol mixing state is closely related to the hygroscopicity (Chen et al., 2022; Fan et al., 2020). Ren et al. (2018) predicted the concentration of CCN using five different mixing state schemes and found that the influence of aerosol mixing state on its activation characteristics ranged from –34% to +16%. Neglecting particle mixing structure can also lead to significant overestimation of the aerosol absorption efficiency (Yao et al., 2022). Therefore, it is important to account for the information of mixing state of ambient particles in climate models so as to reduce the uncertainty in evaluating their environmental and climate effects.

The mixing states of ambient particles are complex. Particles in areas affected by primary emissions are mainly with external mixing state (i.e., the chemical components of particles exist independently), while aerosols in relatively clean areas are mainly transported from

https://doi.org/10.5194/egusphere-2024-2999
Preprint. Discussion started: 24 October 2024

elsewhere and have a higher degree of internal mixing (Swietlicki et al., 2008; Enroth et al., 2018; Chen et al., 2022). Internal mixing typically includes uniform composition or core–shell structures (Jacobson et al., 2001). The former refers to the same proportion of species in any part of the aerosol component, while the latter is defined as the mixing state formed by certain chemical components coating or condensing on the surface of other components during the aging process. Also, the mixing state of particles is variable. Freshly emitted particles undergo various processes, including photochemical and aqueous-phase processes, as well as physical processes such as coagulation and condensation, leading to an increase in their degree of internal mixing. This gradual transition from external to internal mixing characterizes the aging process of particles. The aging timescale varies greatly between clean and polluted areas (Peng et al., 2016; Chen et al., 2017; Ghosh et al., 2021). However, the timescale of aging process of particles was commonly fixed in many models and did not depend on environmental conditions (Chen et al., 2017; Ghosh et al., 2021), which may introduce great uncertainty in the prediction of regional aerosol concentration and the evaluation of aerosol climate effects (Ghosh et al., 2021). Therefore, capturing the temporal scales of the evolution of the aerosol mixing state based on field campaigns is crucial for accurately parameterizing the aging timescale of aerosol particles in models, thereby enhancing the precision of simulations pertaining to the environmental and climatic impacts of aerosols.

At present, some studies have characterized the mixing state and aging process of black carbon (BC) aerosols using different instruments. Transmission electron microscopy (TEM) has been used to determine the mixing state of individual particles in China (Li et al., 2016; Zhang J. et al., 2023). However, based on TEM technique, a large number of aerosol samples

https://doi.org/10.5194/egusphere-2024-2999
Preprint. Discussion started: 24 October 2024

are required so as to make the results with the significance of statistics, which means a high cost both on labors and materials. The most important issue is that the mixing state of particles may change during collection and transportation. Recently, aerosol time-of-flight mass spectrometry (ATOFMAS) and soot-particle aerosol mass spectrometry (SP-AMS) have been used to measure the mixing state of BC and coated aerosol species in real time (Liu et al., 2019; Xie et al., 2020). Overall, previous studies focused more on the mixing state of BC of single-particles (Saha et al., 2018; Xie et al., 2020; Chen et al., 2020). While, the mixing state of particles across a population in ambient atmosphere is more complex (Riemer et al., 2019). For example, aerosols containing two or more components may also exhibit external mixing, as evidenced by the bi- or trimodal distributions of the probability density function of hygroscopic growth factor/hygroscopic parameter (κ) (Gf-PDF; κ-PDF) measured using a humidity tandem differential mobility analyzer (H-TDMA) (Fan et al., 2020; Chen et al., 2022; Zhang S. et al., 2023). The mixing state of particles has been retrieved according to the patterns of Gf-PDF/κ-PDF (Hong et al., 2018; Shi et al., 2022; Spitieri et al., 2023). However, most studies based on the H-TDMA measurements only made qualitative descriptions of the particle mixing state when explaining the variations in the aerosol hygroscopicity (Wang et al., 2019; Chen et al., 2022; Shi et al., 2022).

In this study, with the aim of obtaining insights into the mixing state and aging time scale of ambient particles in urban area, we have identified four different types of size-resolved particles mixing states, and characterized their real-time variations using the field measured hygroscopic growth factor by the H-TDMA in urban Beijing. The dependence of mixing state of particles on temperature (T), relative humidity (RH) and the pollution levels was

https://doi.org/10.5194/egusphere-2024-2999
Preprint. Discussion started: 24 October 2024

investigated. The evolution of mixing state of particles with specific sizes was also explored to imply the timescale of their aging from the diurnal variations during clear and cloudy days. Finally, we compared the aging timescale of aerosol particles with that adopted in current models and other field observations reported in previous literatures.

2 Methods

The campaign was conducted to measure the Gf of particles with different dry sizes (40, 80, 110, 150 and 200 nm) using a H-TDMA from 19 May to 18 June 2017 in Beijing. The instrument used in this study has been described previously (Zhang et al., 2017; Wang et al., 2019; Fan et al., 2020; Chen et al., 2022). Here, we mainly describe the interpretation criteria for the mixing state of particles. The Gf-PDF was obtained by $TDMA_{inv}$ algorithm in this study (Gysel et al., 2009). Then, the κ-PDF of size-resolved particles was retrieved according to the κ-Köhler theory (Petters and Kreidenweis, 2007). Subsequently, we accurately defined four mixing states based on the κ-PDF patterns and the number of peaks in κ-PDF (Figure 1, Figure S1). Given that the freshly emitted hydrophobic particles showed an external mixing state (Li et al., 2016), the κ-PDF, that exhibited only one nearly hydrophobic mode or less hygroscopic (LH; the peak of κ-PDF occurs at $\kappa < 0.1$) mode, was defined as LH external mixing state (type 1). Mixing type 2 indicates that the maximum peak of κ-PDF occurs at LH mode or more hygroscopic (MH, the peak of κ-PDF occurs at $\kappa \geq 0.1$) mode, and the bimodal distributions of the LH and MH modes are present in κ-PDF. Moreover, the κ-PDF pattern with trimodal distributions called transitional external mixing state in this study (type 3). The κ-PDF of type 4 was dominated by MH mode, displaying nearly unimodal patterns, was defined as internal mixing type. In this study, we also calculated the standard deviation of κ-PDF (σ) according to

https://doi.org/10.5194/egusphere-2024-2999
Preprint. Discussion started: 24 October 2024

Spitieri et al. (2023), which indicates the degree of dispersion in the data, and is thought to reflect the mixing degree of particles to a certain extent.

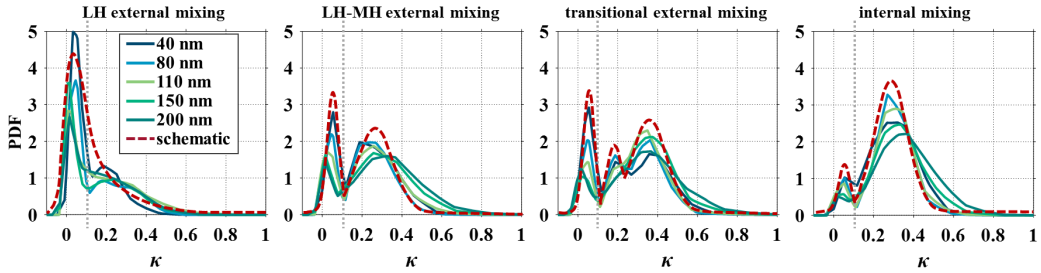

Figure 1. The mean κ-PDF of five particle sizes and the schematic diagram of κ-PDF for four mixing types.

3 Results and discussion

3.1 Overview of the mixing state of size-resolved particles

Figure 2 shows the time series of size-resolved κ, and κ versus σ. The real-time changes in the mixing states of particles are represented by different filled colors. The κ shows large variations in five particle sizes, ranging from 0 to 0.5, accompanied by significant changes in mixing states. In general, the mixing state of particles gradually transitions from external mixing to internal mixing along with increases in κ. For example, particles with size of 40 nm are dominated by LH external mixing and LH-MH external mixing states at κ <0.2; and the transitional external mixing state take up an increasingly proportion often corresponding to κ values of >0.2 and the internal mixing state occurs when κ greater than 0.3 (shown by the light gray dots in Figure 2).

However, there exists different correlations between κ and σ for the five sizes. For particles smaller than 100 nm (i.e., 40 and 80 nm), the σ increases as the κ increases from 0.1 to 0.4, showing a positive correlation. While, the σ for particles larger than 100 nm (i.e., 110,

https://doi.org/10.5194/egusphere-2024-2999
Preprint. Discussion started: 24 October 2024

150 and 200 nm) exhibits a negative trend to κ variations, with the internal mixing and strong particles hygroscopicity but the smaller the value of σ. Our result contrasts with that previously observed in a vegetated site by Spitieri et al. (2023), which used only σ of Gf-PDF as a single indicator to characterize the particles mixing state. Our result indicates that the parameter σ alone cannot characterize the mixing state of particles in megacity of Beijing, where the aerosol particles are usually severely affected by local anthropogenic emissions.

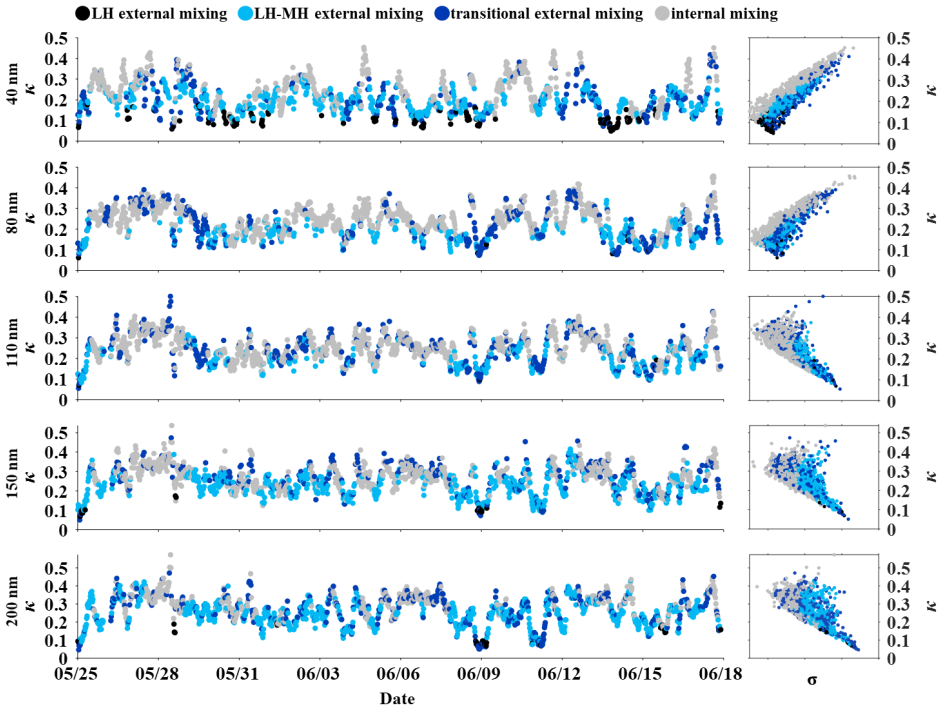

Figure 2. Time series of hygroscopic parameter (κ), and plots of κ versus standard deviation of κ-PDF (σ) for 40, 80, 110, 150 and 200 nm particles (from top to bottom). The colors denote the different mixing types.

The size dependence of mixing type fractions and σ are shown in Figure 3. The external mixing types, including LH external mixing state and LH-MH external mixing state, dominate

https://doi.org/10.5194/egusphere-2024-2999
Preprint. Discussion started: 24 October 2024

in 40, 150 and 200 nm particles, accounting for 47%, 41% and 48% respectively of all mixing types. The elevated fraction in particles with external mixing state is intimately associated with the local sources. For instance, previous study revealed the particle size distribution of aerosols from different sources in urban Beijing, suggesting that the particles with 40 nm predominantly originated from primary emissions, and particles with 150 and 200 nm displayed a strong correlation with transportation sources and biomass burning sources (Ren et al., 2023). Furthermore, for 40 nm particles, besides the impact from primary sources, the relative higher fraction of particles with internal mixing state (37%) is likely due to that the growth and aging process of newly generated particles that are with high hygroscopicity (Wu et al., 2016; Liu et al., 2021a). This is similar to the result observed in Athens, Greece, in which the particles with 30 nm were more internally-mixed (Spitieri et al., 2023). While, for particles with sizes of 80 and 110 nm, the transitional and internal mixing states totally account for 50-80% of all mixing types, corresponding to a significant decrease from about 10% to less than 1% of the fraction of the LH external mixing type. Note that the proportion of transitional external mixing state remains relative constant, with a mean value of 21% across all sizes in this study, implying a continuous influence of atmospheric aging process on the particles mixing state. On average, the result reveals that the externally and internally mixed particles accounted for 56%±12% and 44%±12% respectively. The mixing state of particles derived in this study differs from that reported by Zhang et al., (2017), in which they conducted the measurements at a suburban site of Xinzhou where the aerosols is much less affected by sources nearby, and the aerosols are mainly transported from elsewhere and are thus more aged and well mixed. The result implies that the influence of mixing state on hygroscopicity should be explored at specific particle sizes

https://doi.org/10.5194/egusphere-2024-2999
Preprint. Discussion started: 24 October 2024

due to the heterogeneity of chemical compositions with particle size (Fan et al., 2020, Figure S2).

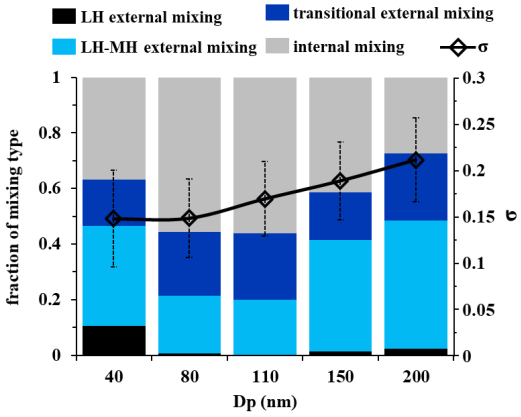

Figure 3. The size dependence of fraction of particles mixing types and σ.

Further, we compared the dependence of κ and σ on the variations of mixing states for five particle sizes (Figure 4). At 40 and 80 nm sizes, it shows that both κ and σ increases markedly when the particles change from external to internal mixing state. While, for particles with sizes of 110, 150 and 200 nm, the σ reduced but the κ increased when the particles change from external to internal mixing state. In other words, the σ of the particles larger than 80 nm shifts to lower values as the particles become more internally mixed. Our results indicate that the standard deviation of κ-PDF alone is insufficient to characterize mixing degree in polluted area.

https://doi.org/10.5194/egusphere-2024-2999
Preprint. Discussion started: 24 October 2024

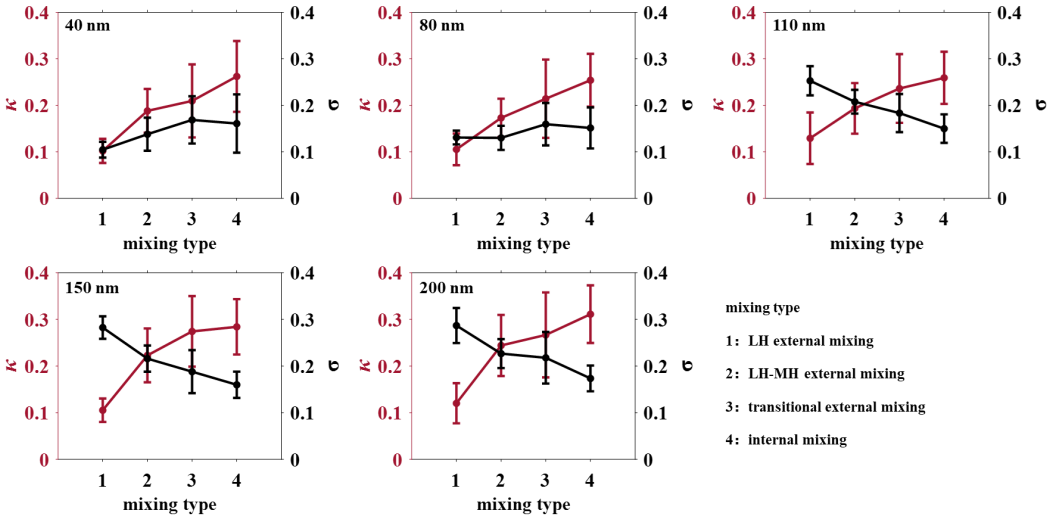

Figure 4. The mixing type dependence of hygroscopicity and σ for five particle sizes.

3.2 Evolution of mixing state of the particles

3.2.1 Diurnal variations

The average diurnal variations of the mixing state and κ of different particle sizes are shown in Figure 5. For 40 nm particles, the fraction of LH external mixing state presents three peaks at morning (9:00–12:00 local time; LT), evening rush hours (18:00–20:00 LT) and nighttime (0:00–03:00 LT). This is accompanied with the impacts from those primary cooking and traffic emissions (Xu et al., 2021; Liu et al., 2021b). Unlike the 40 nm particles, there is no apparent increase of external mixing state for the particles with sizes of 80, 110, 150, 200 nm in the rush hours or cooking times. The results indicate that the particles emitted from local primary sources are small mainly with sizes around 40 nm during the campaign. Correspondingly, the proportion of the particles with internal mixing state was smallest in the morning and nighttime, but exhibiting a rapid increase from about 9:00 until the evening rush hours (about 16:00–18:00). The particles with LH-MH external mixing and transitional

https://doi.org/10.5194/egusphere-2024-2999
Preprint. Discussion started: 24 October 2024

external mixing state represent the intermediate state of the aging process in which particles transition from external mixing to internal mixing, and both showed a decrease to around 10% during the corresponding period of the day as the proportion of particles with internal mixing state increased up to 80%. The diurnal variations imply an apparent aging process that leads the particles changed from external mixing in the early morning to internal mixing in the afternoon. The aging process also changes particles physiochemical properties. As a result, an obvious enhancement in particles hygroscopicity was observed during the daytime, indicating the impact of particles mixing and aging on their hygroscopicity (Hersey et al., 2013; Müller et al., 2017).

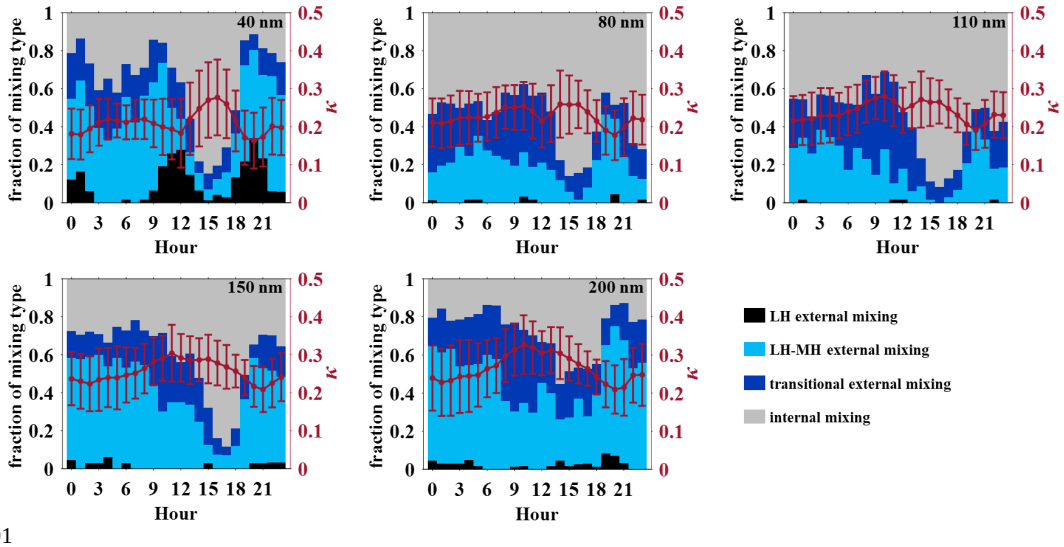

Figure 5. Diurnal variations of the mixing state fraction and κ for five particle sizes.

3.2.2 Dependence of the mixing state on T, RH and PM_1

To elucidate the effect of meteorological condition and particulate pollution level on mixing state of particles, the dependences of particles mixing types on ambient T, RH and PM_1 mass concentrations are further examined (Figure 6). It shows that there is a clear dependence

https://doi.org/10.5194/egusphere-2024-2999
Preprint. Discussion started: 24 October 2024

of mixing state of the particles across all observed sizes on T, for example, for the 40 nm particles, the fraction with external mixing state reduces from 60% to 20%, while that of the internal mixing state increases from 30% to 70% with the increase of T from <20℃ to >35℃. This can be easily explained that the higher ambient T (usually corresponding to the periods in daytime) will generally promote the photochemical aging and mixing of the particles (Riemer et al., 2004; Zhang et al., 2015). But note that, the fraction of particles with internal mixing state decreases evidently when the T increases from 15 ℃ to about 25℃. With the increase of RH from 20% to 80%, the fraction of particles with internal mixing state at 40 nm reduces from 60% to 20%. However, the fraction of the internal mixing state for particles larger than 80 nm is reduced with the increase of RH when its value <60%, while it increases with the RH increase as it larger than 60%, indicating that the very humid atmosphere with high RH is more favorable for particle aging that was reported promoted by the aerosols aqueous process (Zhang et al., 2021).

With the evolution of PM_1 pollution, the fraction of internal mixing state for 40 nm particles significantly decreases to less than 10% due to accumulation of small particles from local primary emissions under heavy pollution conditions, which thus leads to enhanced heterogeneity of particles chemical composition and externally-mixed degree (Fan et al., 2020). While for particles with sizes of 80, 110, 150 and 200 nm, the proportion of internally-mixed state increase to nearly 90% under heavy PM_1 pollution, which is consistent with previous observations in winter of urban Beijing (Chen et al., 2020) and in Xi'an (Wang et al., 2014). Our result implies that those fine aerosol particles experience aging through both the photochemical processes and aqueous growth in the polluted atmosphere of urban Beijing,

https://doi.org/10.5194/egusphere-2024-2999
Preprint. Discussion started: 24 October 2024

thereby affecting their mixing state.

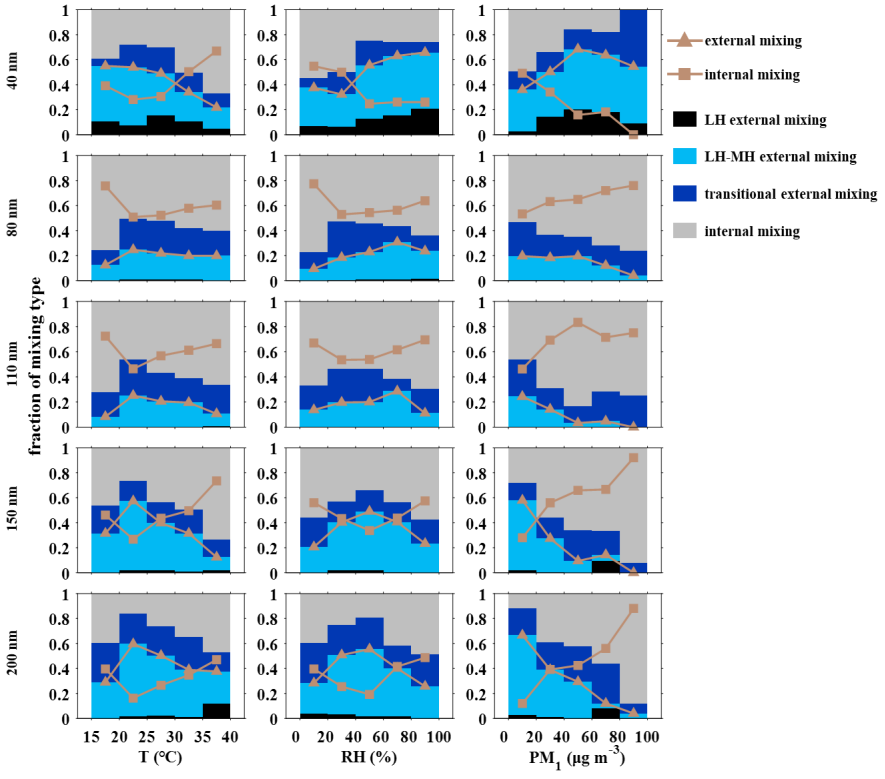

Figure 6. Mixing type fraction as a function of T, RH and PM_1 for five particle sizes. Solid triangles and solid squares represent the fraction of internal and external (LH external mixing + LH-MH external mixing state) mixing states, respectively.

3.3 Particles aging timescale: on clear and cloudy days

Figure 7 shows the average diurnal variations of the fraction of particles with internal mixing state and the mean fractions of all the four mixing types on clear and cloudy days. On clear days, the fraction of internal mixing state increases significantly from ~10-40% before 9:00 to nearly 100% during 12:00–15:00, especially when particle size smaller than 150 nm. While, there is no such notable enhancement on cloudy days. The difference in the proportion

https://doi.org/10.5194/egusphere-2024-2999
Preprint. Discussion started: 24 October 2024

of particles with internal mixing state between the period before 9:00 and during 12:00–17:00 usually does not exceed 50% on cloudy days, and the maximum fractions of particles with internal mixing state on cloudy days were about 50%-90%. Compared with the cloudy days, the fraction of particles with internal mixing for 40 nm is noticeably higher on clear days, which accounts for about 40% of all mixing states, indicating that the 40 nm particles are likely from nucleation processes. On clear days, the particles undergo a gradual shift from external to internal mixing states during 8:00–16:00 accompanied by a growth in particle size from 20 nm to about 100 nm (Figure S3), which is generally 1–2 hours shorter than that observed on cloudy days.

Overall, the aging process is confirmed by the transition of particle from external to internal mixing states, the growth of particle size, and the increase of secondary organic aerosol (Figure S3), which typically spans a duration of approximately 5 to 8 hours, as is similar to the aging timescale of aerosol particles in the polluted Indo-Gangetic Plain (< 10 hours) (Ghosh et al., 2021). Actually, the aerosol particles aging would be largely affected by local atmospheric conditions, and thus would vary both spatially and temporally (Pöschl et al., 2001; Huang et al., 2013). For example, using an environmental chamber approach, Peng et al. (2016) revealed that the timescale of BC aerosols aging is 2.3 and 4.6 hours, 9 and 18 hours over two cities—Beijing and Houston respectively. Note that the faster aging time in Beijing derived in the chamber experiment is probably due to the different levels in the concentration of gaseous precursors. In addition, there is only photochemical aging occurred in the chamber experiment, however, in the atmosphere, the particles aging is also through coagulation process which usually occurs slower than the photochemical reaction and condensation processes (Chen et al.,

https://doi.org/10.5194/egusphere-2024-2999
Preprint. Discussion started: 24 October 2024

2017). This can also explain our observed faster aging time on clear days when the photochemical process is more significant considering that the difference of the pollutant concentrations in daytime between clear and cloudy days is not obvious (i.e., SO_2, NO_2, O_3, PM_1; Figure S4).

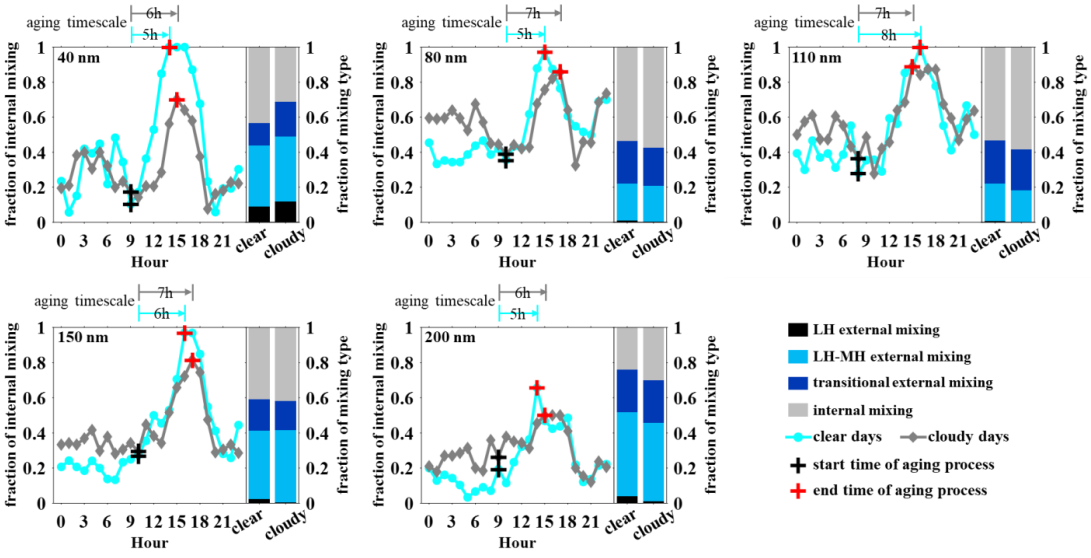

Figure 7. Diurnal variations of internal mixing proportion and statistical results of the fraction of mixing state for five particle sizes on clear and cloudy days. The line segments and time above the graph represent the aging timescale of particles. The start time and end time of particle aging process was selected when the proportion of particles with internal mixing state is closest after sunrise, and when the fraction of internally-mixed particles reaches its maximum, represented by black and red cross respectively.

3.4 Implications to parameterization of the current models

The aging timescale of aerosol significantly impacts their physiochemical properties, which in turn affects their atmospheric lifetime, transport characteristics (Zhang J. et al., 2023) and the direct radiative forcing of aerosol particles (Moffet and Prather, 2009; Wang et al.,

https://doi.org/10.5194/egusphere-2024-2999
Preprint. Discussion started: 24 October 2024

2018). We further compared our results with the results derived from five field sites and the values adopted in current models (Table S1). As shown in Figure 8, the aging timescale of particles in Beijing achieved in this study is 5–8 hours, which is comparable with the observations of that reported in other urban areas like Mexico City (3 hours; Moffet and Prather, 2009) and Los Angeles (3 hours; Krasowsky et al., 2016). The result is also close to the aging timescale of particles in source area of biomass burning in California (4 hours; Akagi et al., 2012). However, the aging time of particles displays large spatial variations at different sites. For example, the aging timescale of particles observed in Beijing (4.6 hours) was four times faster than that in Houston (18 hours) where the precursors concentrations are extremely low (Peng et al., 2016). Overall, the aging time of particles obtained in ambient atmosphere is much shorter than the default values adopted in most models, which is commonly with a duration of 1.15–2.5 days. In addition, the values among different models range greatly from 1 to 20 days (Figure 8). For example, a timescale of 20 days was used to represent a slow aging process (i.e., coagulation) by Liu et al. (2011), as may be not properly applied in regions with high particle number concentration where the particles coagulation is also efficient (Chen et al., 2017).

Although using dynamic parameterization scheme of particles aging in models could achieve the application of different particles aging time to different regions, the simulated values show large variations and uncertainties among different models. For example, in RegCM4 model, the conversion time from fresh to aged BC range from about 5 hours to 7 days (Ghosh et al., 2021). The range in KAMM/DRAIS, however, is only 2 hours to about 1.6 days (Riemer et al., 2004). The aging timescales has been reported ranging from 12 hours to 7 days over central-eastern China based on a regional chemical transport model by Chen et al. (2017),

https://doi.org/10.5194/egusphere-2024-2999
Preprint. Discussion started: 24 October 2024

which is much longer than that derived in urban Beijing by this study.

The large uncertainties in the aging timescale can significantly affect the accuracy of simulation and assessment for atmospheric lifetime, loading and radiation forcing of aerosols. For example, to better simulate the intercontinental transport of aerosols, Huang et al. (2013) implemented a variable aging scheme in the GEOS-Chem model, which showed that the total atmospheric burdens and global average lifetimes of BC (OC, organic carbon) were increase by 8% (2%) compared to the default value (1.15 days). Similarly, due to the implementation of the dynamic aging scheme in models, the column burden and surface mass concentration of carbonaceous aerosols increased during the dry season in the polluted Indo-Gangetic Plain, and the atmospheric heating increased by at least 1.2 W m^{-2} (Ghosh et al., 2021). Therefore, given the large spatiotemporal variations in aging timescale of particles, the study emphasizes the urgency of conducting investigations at more field sites. In addition, the other factors such as the meteorology, aerosol mass loading and particle sizes that affect the aerosols aging should be accounted for so as to improve the dynamic aging schemes in climate models.

https://doi.org/10.5194/egusphere-2024-2999
Preprint. Discussion started: 24 October 2024

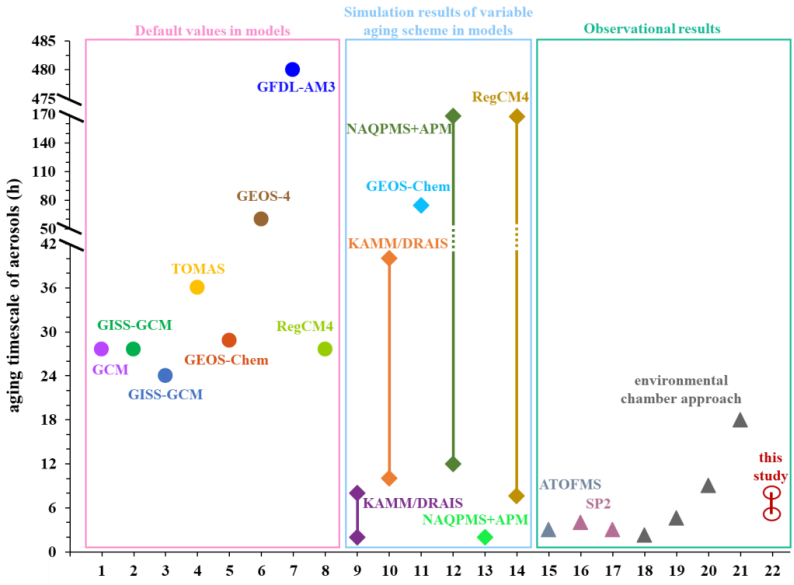

Figure 8. The aging timescale of particles reported in literatures (1. Cooke et al., 2002; 2. Chung and Seinfeld, 2002; 3. Koch and Hansen, 2005; 4. Pierce et al., 2007; 5. Yu and Luo, 2009; 6. Colarco et al., 2010; 7. Liu et al., 2011; 8, 14. Ghosh et al., 2021; 9, 10. Riemer et al., 2004; 11. Huang et al., 2013; 12, 13. Chen et al., 2017; 15. Moffet and Prather, 2009; 16. Akagi et al., 2012; 17. Krasowsky et al., 2016; 18-21. Peng et al., 2016). The solid circle, diamond and the triangle denote the default aging time of particles used in models and stimulation results of variable aging scheme in models, as well as the observational results, respectively.

4 Conclusions

The real-time mixing state of ambient aerosol particles with dry particle sizes of 40, 80, 110, 150 and 200 nm was investigated in urban Beijing, according to PDF of hygroscopic growth factor measured using the H-TDMA system. Four mixing states of ambient size-resolved particles were captured in this study. In general, particles with LH external, LH-MH external, transitional external and internal mixing state account for 0-10%, 20-46%, 17-24%

https://doi.org/10.5194/egusphere-2024-2999
Preprint. Discussion started: 24 October 2024

and 27-56% respectively, which depends on particles size greatly. The diurnal variation of mixing state of particles in all sizes considered present a visible aging process, showing that the fraction of particles with internal mixing state increases significantly from ~10-40% before 9:00 to about 100% during 12:00–15:00 on clear days, accompanied by a growth in particle size from 20 nm to 100 nm, which is more notable than that on cloudy days. Specifically, the aging process of particles within approximately 5–8 hours. In addition, the mixing state of particles was observed to be dependent both on T and RH, showing that the particles with internal mixing state elevates obviously when T or RH exceeds 25°C or 60% respectively. Moreover, with the intensification of particulate pollution, the particles become more internally-mixed. The results indicate that both high ambient temperature and very humid atmosphere are more favorable for particle aging in polluted atmosphere. The large difference of aging timescale of particles between values in models and the timescale achieved by observations, emphasizing the vital role of exploring the aging timescale through more field measurements to improve the accuracy of aging schemes in climate models. The results revealed in our study highlight the considerable impact of atmospheric aging on mixing state of fine aerosol particles in polluted megacities.

Data availability

All data used in the study are available from the corresponding author upon request (zhangfang2021@hit.edu.cn).

https://doi.org/10.5194/egusphere-2024-2999
Preprint. Discussion started: 24 October 2024

Author contributions

FZ and JL conceived the conceptual development of the paper. FZ directed and performed of the experiments with JR, LC and JL. JL conducted the data analysis and wrote the draft. All authors edited and commented on the various sections of the paper.

Competing interests

The authors declare that they have no conflict of interest.

Acknowledgments

This work was funded by the National Natural Science Foundation of China (NSFC) research project (Grant No. 42475112, 42405191), Shenzhen Science and Technology Plan Project (Grant No. GXWD20220811174022002; KCXST20221021111404011), Guangdong Natural Science Foundation (Grant No. 2024A1515011005), Hebei Natural Science Foundation (Grant No. D2024205006). We thank all participants in the field campaigns for their tireless work and cooperation.

Reference

Akagi, S, Craven J, Taylor J, et al. Evolution of trace gases and particles emitted by a chaparral fire in California. Atmospheric Chemistry and Physics, 2012, 12(3), 1397-1421.

Chen X, Wang Z, Yu F, et al. Estimation of atmospheric aging time of black carbon particles in the polluted atmosphere over central-eastern China using microphysical process analysis in regional chemical transport model. Atmospheric Environment, 2017, 163, 44–56.

Chen L, Zhang F, Yan P, et al. The large proportion of black carbon (BC)-containing aerosols in the urban atmosphere. Environmental Pollution, 2020, 263, 114507.

https://doi.org/10.5194/egusphere-2024-2999
Preprint. Discussion started: 24 October 2024

https://doi.org/10.1016/j.envpol.2020.114507

Chen L, Zhang F, Zhang D, et al. Measurement report: Hygroscopic growth of ambient fine particles measured at five sites in China. Atmospheric Chemistry and Physics, 2022, 22, 6773-6786.

Chung S, Seinfeld J. Global distribution and climate forcing of carbonaceous aerosols. Journal of Geophysical Research, 2002, 107(D19), 4407, doi:10.1029/2001JD001397.

Colarco P, Silva A, Chin M, et al. Online simulations of global aerosol distributions in the NASA GEOS-4 model and comparisons to satellite and ground-based aerosol optical depth. Journal of Geophysical Research, 2010, 115, D14207, doi:10.1029/2009JD012820.

Cooke W, Ramaswamy V, Kasibhatla P. A general circulation model study of the global carbonaceous aerosol distribution. Journal of Geophysical Research: Atmospheres, 2002, 107(D16), 10.1029/2001JD001274.

Enroth J, Mikkilä J, Németh Z, et al. Wintertime hygroscopicity and volatility of ambient urban aerosol particles. Atmospheric Chemistry and Physics, 2018, 18, 4533–4548,

Fan X, Liu J, Zhang F, et al. Contrasting size-resolved hygroscopicity of fine particles derived by HTDMA and HR-ToF-AMS measurements between summer and winter in Beijing: The impacts of aerosol aging and local emissions. Atmospheric Chemistry and Physics, 2020, 20(2), 915-929.

Ge S, Su J, Zhao P, et al. Characteristics of $PM_{2.5}$ hygroscopicity and the influences of water-soluble ions during haze events in Beijing. Atmospheric Environment, 2024, 120382.

Ghosh S, Riemer N, Giuliani G, et al. Sensitivity of carbonaceous aerosol properties to the implementation of a dynamic aging parameterization in the regional climate model

https://doi.org/10.5194/egusphere-2024-2999
Preprint. Discussion started: 24 October 2024

RegCM. Journal of Geophysical Research: Atmospheres, 2021, 126, e2020JD033613.

Gysel M, McFiggans GB, & Coe H. Inversion of tandem differential mobility analyser (TDMA) measurements. Journal of Aerosol Science, 2009, 40(2), 134-151.

Hersey SP, Craven JS, Metcalf AR, et al. Composition and hygroscopicity of the los angeles aerosol: CalNex. Journal of Geophysical Research:Atmospheres, 2013, 118(7): 3016-3036.

Hong J, Xu H, Tan H, et al. Mixing state and particle hygroscopicity of organic-dominated aerosols over the Pearl River Delta region in China. Atmospheric Chemistry and Physics, 2018, 18, 14079-14094.

Huang Y, Wu S, Dubey M K, et al. Impact of ageing mechanism on model simulated carbonaceous aerosols. Atmospheric Chemistry and Physics, 2013, 13, 6329–6343.

Jacobson M. Strong radiative heating due to the mixing state of black carbon in atmospheric aerosols. Nature, 2001, 409(6821), 695-697.

Koch D, Hansen J. Distant origins of Arctic black carbon: A Goddard Institute for Space Studies Model experiment. Journal of Geophysical Research, 2005, 110, D04204, doi:10.1029/2004JD005296.

Krasowsky T, McMeeking G, Wang D, et al. Measurements of the impact of atmospheric aging on physical and optical properties of ambient black carbon particles in Los Angeles. Atmospheric Environment, 2016, 142, 496-504.

Liu D, Joshi R, Wang J, et al. Contrasting physical properties of black carbon in urban Beijing between winter and summer. Atmospheric Chemistry and Physics, 2019, 19, 6749–6769.

Liu J, Fan S, Horowitz L, et al. Evaluation of factors controlling long-range transport of black

https://doi.org/10.5194/egusphere-2024-2999
Preprint. Discussion started: 24 October 2024

carbon to the Arctic. Journal of Geophysical Research, 2011, 116, D04307.

Liu J, Zhang F, Xu W, et al. Hygroscopicity of organic aerosols linked to formation mechanisms. Geophysical Research Letters, 2021a, 48, e2020GL091683.

Liu J, Zhang F, Xu W, et al. A large impact of cooking organic aerosol (COA) on particle hygroscopicity and CCN activity in urban atmosphere. Journal of Geophysical Research: Atmospheres, 126, e2020JD033628, 2021b.

Li W, Sun J, Xu L, et al. A conceptual framework for mixing structures in individual aerosol particles. Journal of Geophysical Research: Atmospheres, 2016, 121(22), 13784-13798.

Moffet R, and Prather K. In-situ measurements of the mixing state and optical properties of soot with implications for radiative forcing estimates, Proceedings of the National Academy of Sciences, 2009, 106(29), 11872-11877.

Müller A, Miyazaki Y, Aggarwal S, et al. Effects of chemical composition and mixing state on size-resolved hygroscopicity and cloud condensation nuclei activity of submicron aerosols at a suburban site in northern Japan in summer. Journal of Geophysical Research: Atmospheres, 2017, 122(17), 9301-9318.

Peng J, Hu M, Guo S, et al. Markedly enhanced absorption and direct radiative forcing of black carbon under polluted urban environments. Proceedings of the National Academy of Sciences of the United States of America, 2016, 113(16), 4266–4271.

Petters M D, & Kreidenweis S M. A single parameter representation of hygroscopic growth and cloud condensation nucleus activity. Atmospheric Chemistry and Physics, 2007, 7(8), 1961-1971.

Pierce J, Chen K, Adams P. Contribution of carbonaceous aerosol to cloud condensation nuclei:

https://doi.org/10.5194/egusphere-2024-2999
Preprint. Discussion started: 24 October 2024

processes and uncertainties evaluated with a global aerosol microphysics model. Atmospheric Chemistry and Physics, 2007, 7, 7723-7765.

Pöschl U, Letzel T, Schauer C, et al. Interaction of ozone and water vapor with spark discharge soot aerosol particles coated with benzo[a]pyrene : O_3 and H_2O adsorption, benzo[a]pyrene degradation, and atmospheric implications. Journal of Physical Chemistry A, 2001.

Ren J, Zhang F, Wang Y, et al. Using different assumptions of aerosol mixing state and chemical composition to predict CCN concentrations based on field measurements in urban Beijing. Atmospheric Chemistry and Physics, 2018, 18, 6907-6921.

Ren J, Zhang F, Chen L, et al.Identifying the hygroscopic properties of fine aerosol particles from diverse sources in urban atmosphere and the applicability in prediction of cloud nuclei. Atmospheric Environment, 298, 119615, 2023.

Riemer N, Vogel H, Vogel B. Soot aging time scales in polluted regions during day and night. Atmospheric Chemistry and Physics, 2004, 4 (7), 1885-1893.

Riemer N, Ault A P, West M, et al. Aerosol mixing state: Measurements, modeling, and impacts. Reviews of Geophysics, 2019, 57, 187–249.

Saha P K, Khlystov A, Grieshop A P. Downwind evolution of the volatility and mixing state of near-road aerosols near a US interstate high way. Atmospheric Chemistry and Physics, 2018, 18(3): 2139-2154.

Shi J, Hong J, Ma N, et al. Measurement report: On the difference in aerosol hygroscopicity between high and low relative humidity conditions in the North China Plain. Atmospheric Chemistry and Physics, 2022, 22, 4599-4613.

https://doi.org/10.5194/egusphere-2024-2999
Preprint. Discussion started: 24 October 2024

Spitieri C, Gini M, Gysel-Beer M, et al. Annual cycle of hygroscopic properties and mixing state of the suburban aerosol in Athens, Greece. Atmospheric Chemistry and Physics, 2023, 23, 235-249.

Swietlicki E, Hansson H C, Hameri K, et al. Hygroscopic properties of submicrometer atmospheric aerosol particles measured with H-TDMA instruments in various environments - a review. Tellus B, 2008, 60, 432-469.

Wang Q, Huang R J, Cao J, et al. Mixing State of Black Carbon Aerosol in a Heavily Polluted Urban Area of China: Implications for Light Absorption Enhancement. Aerosol Science and Technology, 2014, 48:7, 689-697.

Wang Y, Li Z, Zhang R, et al. Distinct ultrafine- and accumulation-mode particle properties in clean and polluted urban environments. Geophysical Research Letters, 2019, 46, 10,918–10,925.

Wang Y, Ma P, Peng J, et al. Constraining ageing processes of black carbon in the community atmosphere model using environmental chamber measurements. Journal of Advances in Modeling Earth Systems, 2018, 10, 2514–2526.

Wu Z J, Zheng J, Shang D J, et al. Particle hygroscopicity and its link to chemical composition in the urban atmosphere of Beijing, China, during summertime. Atmospheric Chemistry and Physics, 2016, 16(2), 1123–1138.

Xu W, Chen C, Qiu Y, et al. Size-resolved characterization of organic aerosol in the North China Plain: new insights from high resolution spectral analysis. Environmental Science: Atmospheres, 2021, 1(6), 346–358.

Xie C, He Y, Lei L, et al. Contrasting mixing state of black carbon-containing particles in

https://doi.org/10.5194/egusphere-2024-2999
Preprint. Discussion started: 24 October 2024

summer and winter in Beijing. Environmental Pollution, 2020, 263, 114455.

Yao Y, Curtis J, Ching J, et al. Quantifying the effects of mixing state on aerosol optical properties. Atmospheric Chemistry and Physics, 2022, 22, 9265-9282.

Yu F, Luo G. Simulation of particle size distribution with a global aerosol model: contribution of nucleation to aerosol and CCN number concentrations. Atmospheric Chemistry and Physics, 2007, 9, 10597-10645.

Zhang S, Shen X, Sun J, et al. Atmospheric Particle Hygroscopicity and the Influence by Oxidation State of Organic Aerosols in Urban Beijing. Journal of Environmental Sciences, 2023, 124, 544-556.

Zhang F, Wang Y, Peng J, et al. Uncertainty in Predicting CCN Activity of Aged and Primary Aerosols. Journal of Geophysical Research: Atmospheres, 2017, 122, 11723–11736.

Zhang J, Liu J, Tao S, et al. Long-range transport of black carbon to the Pacific Ocean and its dependence on aging timescale, Atmospheric Chemistry and Physics, 2015, 15(20), 11521-11535.

Zhang J, Li W, Wang Y, et al. Structural collapse and coating composition changes of soot particles during long-range transport. Journal of Geophysical Research: Atmospheres, 2023, 128, e2023JD038871.

Zhang Y, Liu H, Lei S, et al. Mixing state of refractory black carbon in fog and haze at rural sites in winter on the North China Plain. Atmospheric Chemistry and Physics, 2021, 21, 17631–17648.